Structural, Morphological and Electrical Properties of TiO_2 Thin Films Deposited by ALD Method

Seung-Yeon Oh[*], Jae-Min Shin[*], Gyeong-Hun Na[*], Min-Seok Kwon[**], Sang-Jeen Hong[***] and Bumsuk Jung[*†]**

[*]Department of Electronic Engineering, Myongji University,
[**]Department of Electrical Engineering, Myongji University,
[***†] Department of Semiconductor Engineering, Myongji University

ABSTRACT

TiO_2 thin films were grown using the Atomic Layer Deposition (ALD) and their structural and electrical properties were investigated. The crystal structure, dielectric constant, and surface roughness of the TiO_2 thin films grown by the ALD deposition method were studied. The grown TiO_2 thin films showed an anatase crystal structure, and their properties varied with temperature. In particular, the properties of the TiO_2 thin films were confirmed by changing the process temperature. The electrical properties of Metal-Insulator-Silicon (MIS) capacitor structures were analyzed using a probe station. The performance improvement of capacitors using TiO_2 as a dielectric was confirmed by measuring capacitance through Capacitance-Voltage (C-V) curves.

Key Words : Thin Film, Dielectric Layer, Titanium Dioxide

1. Introduction

The issue faced during the shrink process in DRAM is maintaining capacitance while scaling down its size. To achieve this, there are methods that focus on increasing the area of the capacitor by either increasing its height or enhancing the dielectric material's permittivity. However, increasing the height of the capacitor to enlarge its area is challenging and can raise the difficulty of the fabrication process. Therefore, in this case, research has been conducted on enhancing the permittivity of the dielectric material to increase capacitance. [1]

Among the high-k materials, TiO_2 was chosen for being one of the promising materials for the dielectric layer in next-generation capacitors due to its high permittivity than ZrO_2 and HfO_2, which are currently used in mass production in the study. [2] The $ZrO_2/Al_2O_3/ZrO_2$ (ZAZ) stack, which currently serves as the capacitor dielectric in commercialized DRAM, offers a minimum equivalent oxide thickness (EOT) of approximately 0.6 nm. However, according to the international technology roadmap for semiconductors, a smaller EOT (down to 0.3 nm) with a leakage current density of less than 10^{-7} A/cm$_2$ at a capacitor voltage of 0.6 V will soon be required for DRAM with a design rule of less than 20 nm. ZAZ is not expected to fulfill these requirements due to its insufficient k values. [3] The increasing integration of semiconductors has raised the need not only for the research and development of high-k materials but also for the advancement of fine patterning techniques. In response to this, TiO_2 is being considered as a spacer patterning material in the self-aligned double patterning (SADP) technique.[4] Bulk TiO_2 exhibits crystal structures such as brookite, anatase, and rutile, and it possesses a very high dielectric constant ranging from approximately 16 to 100. [5-6]

ALD is a Chemical Vapor Deposition (CVD) technique that deposits thin films based on the self-limiting reaction between precursor species. ALD allows precise control of film thickness at the atomic layer level and exhibits superior step coverage and aspect ratio compared to conventional

[†]E-mail: bjung@mju.ac.kr

CVD and Physical Vapor Deposition (PVD) methods. In addition, ALD can be performed at relatively low temperatures below 300°C, in contrast to CVD, making it applicable to various substrates, including organic and plastic materials that can withstand low-temperature processes. [7]

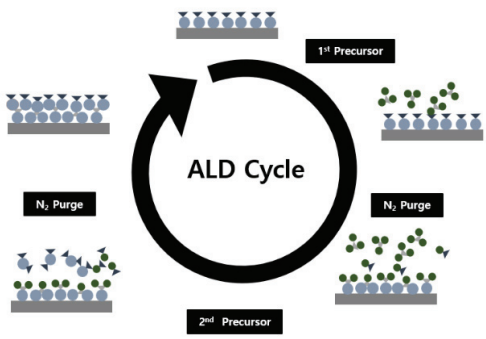

Fig. 1. ALD Cycle.

When the process temperature is lower than the defined ALD window, rapid Growth Per Cycle (GPC) can occur due to the adsorption and condensation of precursor species on the substrate surface or due to reduced reactivity and slow material transport caused by low thermal energy supply, leading to a decrease in deposition rate.

Due to precursor decomposition, the self-limiting reaction on the substrate surface is hindered, resulting in an increase in GPC and a CVD-like growth with longer process times at higher temperatures than the ALD window. Furthermore, at higher process temperatures, adsorbed precursors can desorb or deposited single films can decompose, leading to a decrease in GPC. Fig. 2 shows the ALD window for Titanium Tetra Isopropoxide (TTIP) and H_2O, which is approximately in the range of 190-250°C. [8]

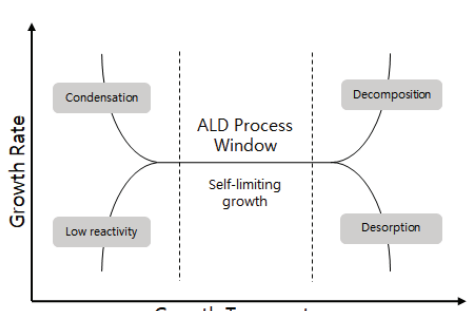

Fig. 2. ALD Window.

Therefore, we varied the process temperature at 150°C, 200°C, and 250°C to observe the anatase crystal structure and analyze the characteristics of the TiO_2 thin films with respect to temperature.

2. Experimental

2.1 Experiment Process

The ALD equipment used in this study, Lucida D100, adopts the travel wave method, which features a lateral type structure where the reactive gases flow laterally through a distributor. As a result, a common trend of higher thickness in the right region of the wafer compared to the left region was observed, as depicted in Fig.3.[9]

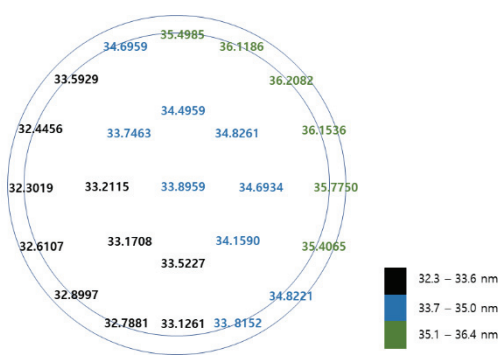

Fig. 3. 1100cycles 250°C film thickness with Ellipsometer.

A 4-inch low-resistance p-type (100) silicon wafer with a resistivity of 0.01-0.02 Ωcm was subjected to cleaning using BOE (Buffered Oxide Etchant) to remove the oxide layer. $TiCl_4$ is very reactive when a chemical reaction occurs with H_2O, however it produces by-product HCl which is highly corrosive.[10] TTIP was used as the precursor in the experiment, as it has the highest vapor pressure among the titanium alkoxide series.[11] The storage canister for the precursor was set at 70°C, the temperature of the reaction material H_2O was 8°C, and the carrier gas N_2 was set at 80 standard cubic centimeter per minute(sccm). The assist pulse for smooth supply of the TTIP precursor was set to 0.2 seconds, the TTIP pulse was set to 0.5 seconds, purge was set to 20 seconds, the H_2O pulse was set to 0.3 seconds, and H_2O purge was set to 20 seconds.

The thickness of the TiO_2 film was measured using an ellipsometer. TiO_2 films were deposited at 150°C, 200°C,

and 250°C with 1100 cycles each, and their thicknesses were measured using an ellipsometer. The GPC values were calculated as 0.019 nm/cycle at 150°C, 0.02 nm/cycle at 200°C, and 0.03 nm/cycle at 250°C. To deposit approximately 30 nm in this experiment, the cycle numbers were set to 1571 cycles at 150°C, 1515 cycles at 200°C, and 1100 cycles at 250°C.

To control the organic contamination on the surface after TiO_2 deposition, organic cleaning was performed. After that, aluminum for the MIS structure was deposited using e-beam evaporation to a thickness of approximately 500 nm. Next, photolithography was carried out to create an island structure. Positive Photoresist (PR) was used, and it was spun at 4500 rpm for 40 seconds to achieve a PR thickness of about 2 μm. Then, a sequence of processes including soft bake at 90°C for 90 seconds, exposure, Post-Exposure Bake (PEB) at 110°C for 60 seconds, development using Tetramethylammonium hydroxide (TMAH), and hard bake at 120°C for 90 seconds was performed for the photolithography process. Following that, Al wet etching using APAl-1 solution was carried out for approximately 10 minutes to complete the island structure. Afterward, PR stripping using acetone was performed, and the completion of Al etching was verified using a surface profiler.

For the creation of radial and square pattern samples, dicing was performed after the fabrication of the MIS structure to divide them into halves. Dicing can result in the deposition of carbon debris(particles) on the sample surface due to the blade, so a protective PR layer was used to prevent this, followed by dicing and PR stripping.

2.2 Experimental measurement

2.2.1 Ellipsometer

Measurements were performed using the Elli-SE-UaM8 ellipsometer from Ellipso Technology. An ellipsometer is a device used to measure the optical properties of thin films, such as thickness and refractive index. It utilizes two orthogonal plane waves that propagate in directions perpendicular to each other to measure the refractive index and thickness of the thin film. By employing two orthogonal linear waves perpendicular to the propagation direction, an ellipsometer measures the optical responses, including refraction, reflection, and absorption, occurring at the thin film surface. In other words, it measures the amplitude and phase changes of the waves generated when they interact with the thin film surface, providing information about the film's thickness, refractive index, surface roughness, and other characteristics.

2.2.2 X-ray Photoelectron Spectroscopy (XPS)

For XPS analysis, TiO_2 thin films were deposited using the DISCO DFD6340 at 250°C for 1100 cycles and diced into 1cm x 1cm size samples. The XPS analysis was performed using the NEXSA instrument from ThermoFisher Scientific. Before analysis, a 60-seconds etching process at 500eV was carried out to achieve accurate surface composition analysis. The X-ray spot size used was 400μm.

2.2.3 Grazing Incidence X-ray Diffraction (GIXRD)

For thin film structural analysis, the Rigaku SmartLab instrument was used to perform GIXRD instead of conventional XRD. GIXRD differs from XRD by fixing the incident angle and adjusting only the detector angle to examine crystallographic properties. This allows for reducing unwanted peaks from the silicon wafer and selectively extracting the peaks related to the thin film. GIXRD also offers approximately three times higher X-ray intensity compared to XRD and provides improved detection of trace elements and crystallinity compared to XRD. It was reported that the measurement of the anatase peak was successful when the incident angle was set at 0.29 degree.[12] Therefore, in this study, the incident angle was set to 0.3degree.

2.2.4 Atomic Force Microscope (AFM)

AFM is a device used to analyze the surface of a sample, where forces such as friction and attraction act between the cantilever tip and the surface depending on the distance. AFM is divided into three modes depending on the type of force acting, and in this study, tapping mode was utilized. Tapping mode utilizes the natural oscillation frequency of the cantilever tip material to vibrate the tip and analyze the surface, minimizing damage to the sample surface. Anton Paar's AFM equipment was used to analyze the surface with a size of 5 μm x 5 μm.

2.2.5 Field Emission Scanning Electron Microscopy (FE-SEM)

SEM operates on the same principle as an optical microscope, using electrons with high energy instead of

light. However, the resolution of an optical microscope is limited by the wavelength, whereas accelerated electrons have short wavelengths, allowing observation of very small features.[13]

When analyzing the 150°C sample, ion sputtering was performed by coating with 1 nm of Pt for 100 seconds due to low conductivity. The measurements were conducted using a Hitachi SU-70 equipment with the following settings: Accelerating Voltage = 15000V, Condition = Vacc = 15 kV, WD = 5 mm.

2.2.6 Photomask

A 127 mm x 127 mm 5-inch square mask was fabricated. When a TiO_2 film of approximately 20 nm thickness had an accumulation capacitance of 110 pF on a metal pad with an area of 100 μm × 100 μm, an effective dielectric constant of approximately 65 was obtained.[14] Therefore, circular photomasks were fabricated with diameters of 100 μm, 200 μm, 300 μm, and 400 μm, respectively as depicted in Fig. 4.

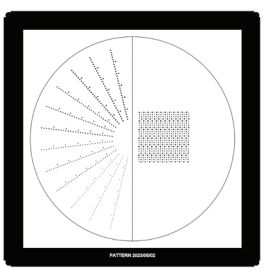

Fig. 4. Photomask pattern.

3. Results and Discussion

Fig. 5 shows a cross-section of a 30nm thick TiO_2 film deposited on the center region at 250°C, analyzed using FE-SEM. The surface of the TiO_2 film grown at 250°C appears to be uniform. Furthermore, by performing clipping using a diamond tip, it can be observed that cracks occurred in the Al region.

The characteristics of the TiO_2 film deposited at different temperatures were analyzed using XPS, GIXRD, AFM, Probe Station, and FE-SEM.

XPS was performed to analyze the composition of the deposited TiO_2 film before analyzing its characteristics at different temperatures. In Fig. 6, the XPS analysis results of the TiO_2 film deposited at 250°C are presented. The narrow scan spectrum of the O 1s core level peak in Fig. 6(a) showed a binding energy of 530.34 eV. In Fig. 6(b), the XPS narrow scan spectrum of the Ti 2p core level revealed the binding energies of the main peaks, Ti 2p1/2 at 464.28 eV and Ti 2p3/2 at 458.81 eV, indicating the presence of quantifiable TiO_2 species formed at a deposition temperature of 250°C. When analyzing the O1s peak at 150°C and 200°C, it was found to correspond to the O 1s peak associated with O_2- bonded to Ti^{4+} at 530.3 eV [15]. In Fig. 6(c), the XPS Ti 2p spectrum of the deposited TiO_2 film showed the presence of Ti 2p3/2 and Ti 2p1/2 peaks at 458.81 eV and 464.28 eV, respectively, in all samples, confirming their alignment with the Ti^{4+} positions in TiO_2. [16] The peak at 284.5 eV corresponds to the C=C bond.[17]

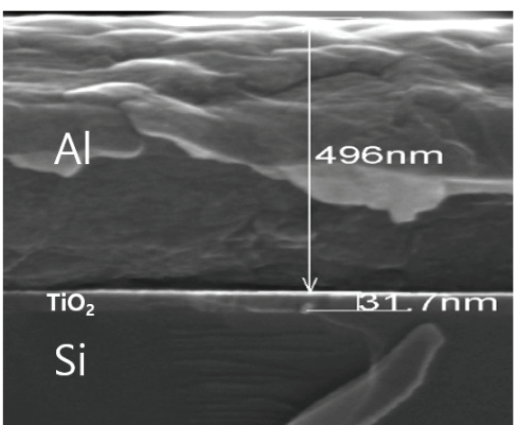

Fig. 5. 250°C MIS structure using FE-SEM.

GIXRD was used to determine the angle of the anatase peak of the TiO_2 film by comparing it with the ICDD card (01-070-6826), which provides diffraction and crystallographic data for various materials. From the intensity shown in Fig. 7, at same ALD cycle, it can be observed that at a process temperature of 150°C, no matching peak was observed. In conclusion at 200°C, weak anatase peaks were observed at approximately 37.21 and 38.76 degrees, while a strong anatase peak was observed at 25.42 degrees for a process temperature of 250°C.

As shown in Fig. 8, it can be observed that when the thickness is fixed at 30nm, the anatase peak intensity at 200°C (25.52, 38.95, 48.33, 55.28 degrees) was found to be higher than at 250°C (25.55, 38.08, 48.34, 54.24, 55.38 degrees) with a higher number of cycles. [18]

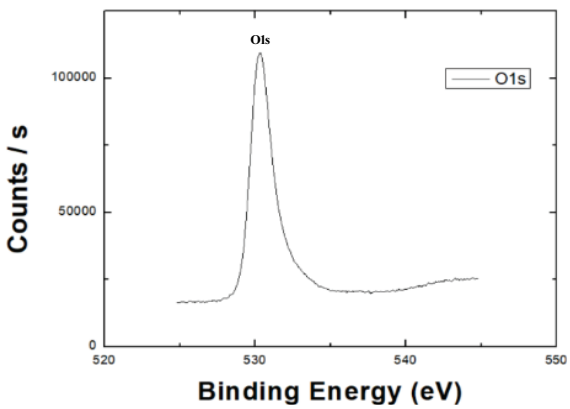

(a)

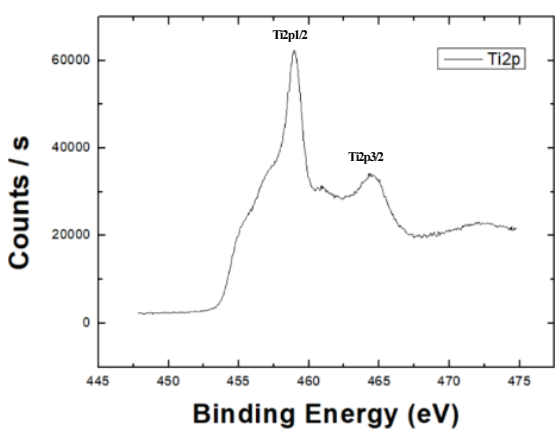

(b)

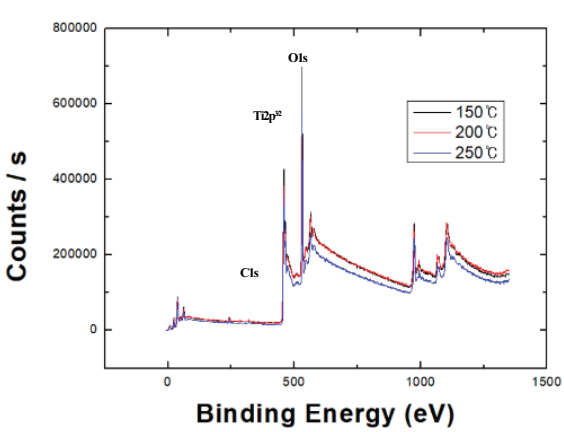

(c)

Fig. 6. XPS spectra showing the chemical composition of TiO_2 films deposited at 150°C, 200°C, 250°C (a) O1s, (b) Ti2p, (c) XPS survey (narrow scan spectrum)

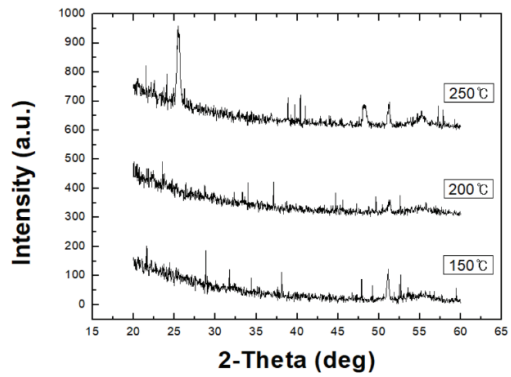

Fig. 7. GIXRD at 150°C, 200°C, 250°C at 1100 cycles.

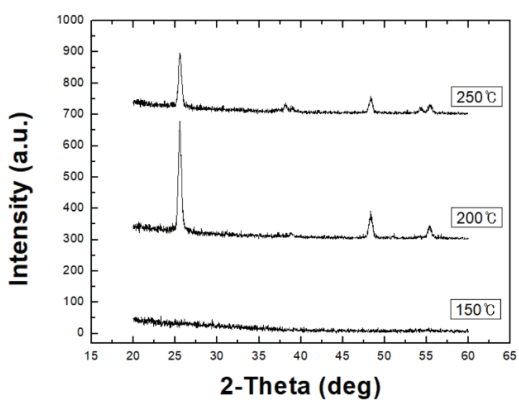

Fig. 8. GIXRD at 150°C, 200°C, 250°C at 30nm.

Fig. 9 shows the AFM analysis results for film crystallinity and surface roughness. It can be observed that the Root Means Square (RMS) surface roughness increases with an increase in the process temperature. Moreover, the crystallinity becomes more pronounced with increasing temperature, indicating that the process temperature affects the surface roughness. The AFM analysis revealed an RMS surface roughness of approximately 0.3 nm for the amorphous film deposited at 150°C. For amorphous films, the deposition follows the crystal direction of the bare wafer, resulting in a similar surface roughness. In addition, the RMS surface roughness of the film deposited at 200°C is lower compared to the film deposited at 250°C, which can be attributed to the formation of densely packed nanocrystalline particles.[19] The AFM measurements yielded RMS values of 0.318 nm at 150°C, 1.667 nm at 200°C, and 2.206 nm at 250°C, with the RMS value at 200°C being larger than that at 250°C. This is attributed to the dominance

of the hydrolysis reaction at 200°C, resulting in a higher RMS value at that temperature.[20]

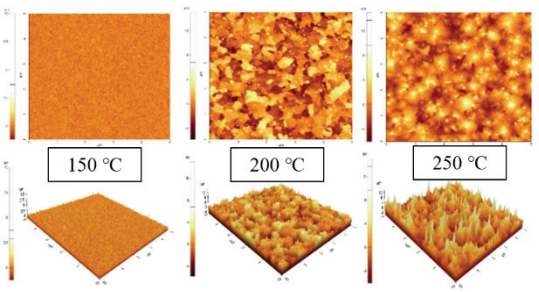

Fig. 9. AFM at 150°C, 200°C, 250°C.

The average grain size of all samples was determined using SEM images at 150, 200, 250°C. At 150°C, the bright region with high contrast corresponds to the area where Pt is deposited, while the dark region represents the original surface where Pt is not deposited. For samples deposited at 150°C, the grains are observed to be spherical in shape. Similarly, for samples deposited at 200°C and 250°C, the grains are found to be densely packed in a planar configuration as shown in Fig. 10.

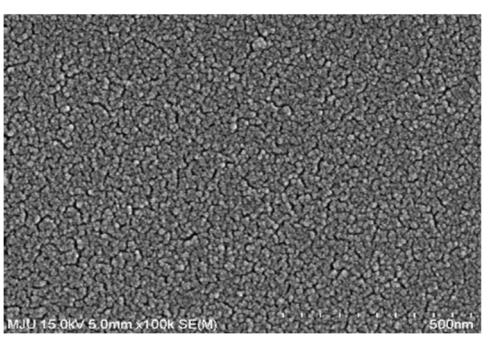

(a)

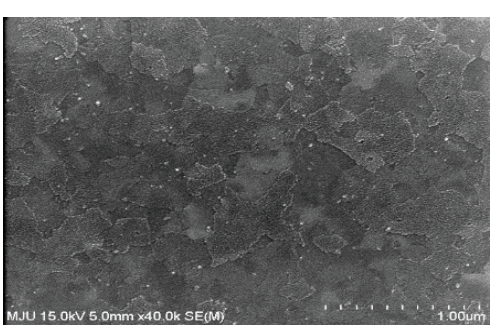

(b)

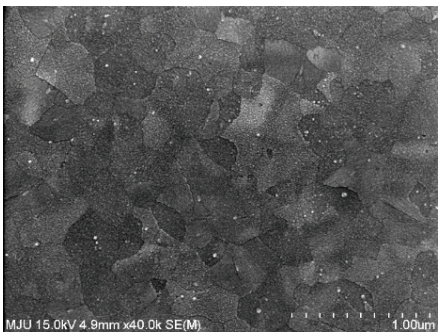

(c)

Fig. 10. TiO_2 surface examination with SEM (a) 150°C, (b) 200°C, (c) 250°C.

To measure the capacitance and leakage current of TiO_2 thin films, a Keithley 4200-SCS Parameter Analyzer was utilized. As the process temperature increased from 150°C to 200°C and 250°C in the TiO_2 accumulation region, the capacitance exhibited an increase shown in Fig. 11.

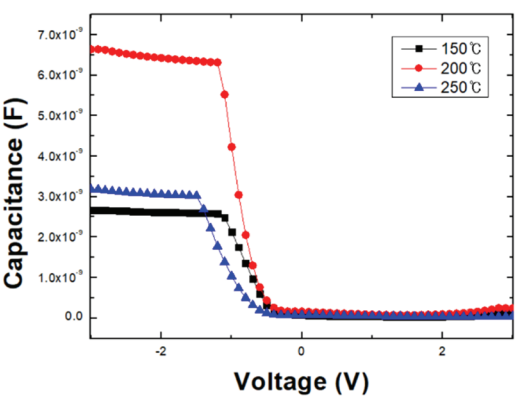

Fig. 11. C-V characteristics as a function of process temperature for 200 μm pattern size.

In Fig. 12, the capacitance was measured while the process temperature was fixed to 250°C and varying the frequency from 500KHz to 10MHz. The capacitance value appeared to be higher as the frequency increase.[21]

Crystal size was calculated using the Debey-Scherrer equation and the results were written in Table 1,2. It is observed that the crystal size is relatively larger at 250°C compared to 200°C, which leads to the formation of more grain boundaries at 200°C than at 250°C. Consequently, it is determined that these increased grain boundaries at 200°C have influenced the higher leakage current, as depicted in Fig. 13.[22]

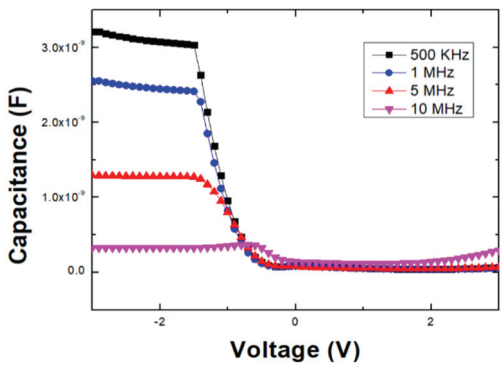

Fig. 12. C-V characteristics as a function of frequency at 250°C for 100 μm pattern size.

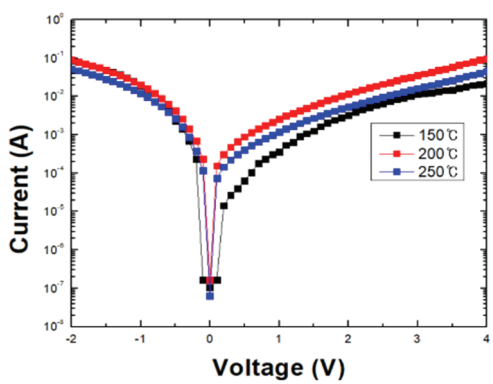

Fig. 13. I-V characteristics as a function of process temperature for 100 μm pattern size.

In Fig. 8, it is observed that the anatase (101) peak at 200°C exhibits a higher intensity compared to that at 250°C. This indicates a better formation of crystalline material, providing information about the directionality and density of the crystal structure. The relatively high capacitance value at 200°C is attributed to the increased crystallinity.[23]

Table 1. Phase, FWHM, Crystal size at 200°C

2θ(°)	Phase name	FWHM(°)	Crystal size(nm)
25.522	Anatase, syn: 101	0.411	20.69
38.95	Anatase, syn: 004	1.2	7.33
48.33	Anatase, syn: 200	0.49	18.55
55.28	Anatase, syn: 105	0.49	19.11

Table 2. Phase, FWHM, Crystal size at 250°C

2θ(°)	Phase name	FWHM(°)	Crystal size(nm)
25.548	Anatase, syn: 101	0.420	20.25
38.08	Anatase, syn: 004	0.39	22.50
48.34	Anatase, syn: 200	0.45	20.20
54.24	Anatase, syn: 105	0.45	20.71
55.38	Anatase, syn: 211	0.48	19.52

Table 3. Summary of thickness, composition, RMS, and capacitance at 150°C, 200°C, 250°C

	Thickness	Composition (Ti2p/O1s)	RMS	Capacitance
150°C	30 nm	34.96/65.04 %	0.318 nm	2.67 nF
200°C	34 nm	35.99/64.01 %	1.667 nm	6.64 nF
250°C	35 nm	36.08/63.92 %	2.206 nm	3.18 nF

4. Conclusions

The capacitance characteristics of TiO_2 thin films for dielectric layers in DRAM capacitors were analyzed by varying the process temperature by ALD. XRD and SEM analyses indicated that while the film was amorphous at 150°C, increasing the process temperature resulted in increased crystallinity, with the films exhibiting an anatase structure and larger grain sizes. XRD and AFM analyses also indicate as the crystallinity increases, the RMS surface roughness increases.

Through this experiment, we confirmed an increase in capacitance value with an increase in process temperature in the accumulation region.

While we investigated the gradual upward trend of capacitance with respect to process temperature, the changes in dielectric properties are influenced by various factors such as the impurity content within the oxide, interfacial properties between the thin film, oxide density, and crystallinity. Therefore, in order to compare more precise dielectric values at each process temperature, further studies and experiments are required.

Acknowledgement

This research was conducted as part of the 2023 Department-Industry Cooperative Semiconductor Major Track Program, supported by the Korea Institute for Advancement of technology (Project No. G02P18800005501). We would like to express our gratitude to Professor Tae Min Ha from the Semiconductor Process Diagnosis Research Center at Myongji University for his mentoring and valuable assistance throughout the research process.

References

1. J. G. Bang, J. H. Lee, E. C. Do, H. J. Kim, B. H. Na, H. R. Kim, B. E. Park, J. H. Lee, C. H. Kim, H. W. Jang, Y.

S. Kim, “Interface engineering for substantial performance enhancement in epitaxial all-perovskite oxide capacitors”, *NPG Asia Mater.*, vol. 15, no. 4, pp. 1-7, 2023. [DOI:10.1038/s41427-022-00460-x]

2. K. H. Yim, Y. Yong, J. H. Lee, K. H. Lee, H. H. Nahm, J. H. Yoo, C. H. Lee, C. S. Hwang, S. W. Han, “Novel high-κ dielectrics for next-generation electronic devices screened by automated ab initio calculations”, *NPG Asia Mater.,* vol. 7, pp. 190-e190, 2015. [DOI: 10.1038/am.2015.57]
3. Jeon, W., Rha, S. H., Lee, W., Yoo, Y. W., An, C. H., Jung, K. H. and Hwang, C. S., “Controlling the Al-doping profile and accompanying electrical properties of rutile-phased TiO2 thin films” *ACS Appl. Mater. & interfaces*, vol. 6, no. 10, pp. 7910-7917, 2010. [DOI: /10.1021/am501247u]
4. Raley, A., Thibaut, S., Mohanty, N., Subhadeep, K., Nakamura, S., Ko, A. and Biolsi, P., “Self-aligned quadruple patterning integration using spacer on spacer pitch splitting at the resist level for sub-32nm pitch applications”, *In Advanced Etch Technology for Nanopatterning V*, vol. 9782, pp. 30-43, 2016. [DOI: 10.1117/12.2219321]
5. Kittl, J. A., Opsomer, K., Popovici, M., Menou, N., Kaczer, B., Wang, X. P., ... & Wouters, D. J., “High-k dielectrics for future generation memory devices.”, *Microelectron. Eng.*, vol. 86, no. 7-9, pp. 1789-1795, 2009. [DOI:10.1016/j.mee.2009.03.045]
6. Dang, V. S., Parala, H., Kim, J. H., Xu, K., Srinivasan, N. B., Edengeiser, E., ... & Devi, A., “Electrical and optical properties of TiO_2 thin films prepared by plasma-enhanced atomic layer deposition”, *Phys. status solidi (a)*, vol. 211, no. 2, pp. 416-424, 2009. [DOI:10.1002/pssa.201330115]
7. K. J. Yoon and O. S. Song, “Property of the Nano-Thick TiO_2 Films Using an ALD at Low Temperature”, Korean Journal of Materials Research, vol. 18, no. 10, pp. 515, 2008. [DOI: 10.3740/MRSK.2008.18.10.515]
8. Reinke, M., Kuzminykh, Y., & Hoffmann, P., “Surface reaction kinetics of titanium isopropoxide and water in atomic layer deposition”, *J. Phys. Chem. C*, vol. 120, no. 8, pp. 4337-4344, 2016. [DOI: 10.1021/acs.jpcc.5b10529]
9. George, Steven M. "Atomic layer deposition: an overview." *Chem. Rev.* vol. 110, no. 1, pp. 111-131, 2010. [DOI: 10.1021/cr900056b]
10. Armstrong C., Delumeau L. V., Munoz-Rojas D., Kursumovic A., MacManus-Driscoll J. and Musselman K. P., “Tuning the band gap and carrier concentration of titania films grown by spatial atomic layer deposition: a precursor comparison”, Nanoscale Advances, vol. 3, no. 20, pp. 5908-5918, 2021. [DOI: 10.1039/d1na00563d]
11. Ritala, M., Leskela, M., Niinisto, L., Haussalo, P., “Titanium isopropoxide as a precursor in atomic layer epitaxy of titanium dioxide thin films”, *Chem. Mater.*, vol. 5, no. 8, pp. 1174-1181, 1993. [DOI: doi.org/10.1021/cm00032a023]
12. Chiappim, W., Testoni, G. E., Moraes, R. S., Pessoa, R. S., Sagás, J. C., Origo, F. D., Maci & Maciel, H. S., “Structural, morphological, and optical properties of TiO_2 thin films grown by atomic layer deposition on fluorine doped tin oxide conductive glass”, *Vacuum*, vol. 123, pp. 91-102, 2016. [DOI: 10.1016/j.vacuum.2015.10.019]
13. A. Alyamani and O. M. Lemine. "FE-SEM characterization of some nanomaterial." *Scan. electron Microsc.*, 2012. [DOI: 10.5772/34361]
14. D. H. Shin, H. L. Cho, S. R. Park, H. J. Oh, and D. H. Ko, “Improvement in Capacitor Characteristics of Titanium Dioxide Film with Surface Plasma Treatment”, *J. Semicond. & Displ. Technol*, vol. 18, no. 1, pp. 32-37, 2019.
15. Kaufherr, N. and Lichtman, D., “X-ray photoelectron spectroscopy studies of thin films of TiN x having different annealing histories” *J. Vac. Sci. & Technol. A: Vacuum, Surfaces, and Films*, vol. 3, no. 5, pp. 1969-1972, 1985. [DOI: 10.1116/1.572953]
16. Bharti, B., Kumar, S., Lee, H. N. and Kumar, R., “Formation of oxygen vacancies and Ti3+ state in TiO_2 thin film and enhanced optical properties by air plasma treatment”, *Sci. Rep.*, vol. 6, no. 1, pp. 1-12, 2016. [DOI: 10.1038/srep32355]
17. Y. Li, J. Shen, J. Li, S. Liu, D. Yu, R. Xu, W. F. Fu, X. J. Lv, “Constructing a novel strategy for carbon-doped TiO_2 multiple-phase nanocomposites toward superior electrochemical performance for lithium ion batteries and the hydrogen evolution reaction”, *J. Mater. Chem. A*, vol. 5, no. 15, pp. 7055-7063, 2017. [DOI: 10.1039/C7TA01184A]
18. Dirnstorfer, I., Mähne, H., Mikolajick, T., Knaut, M., Albert, M., & Dubnack, K., “Atomic layer deposition of anatase TiO_2 on porous electrodes for dye-sensitized solar cells” *J. Vac. Sci. & Technol. A: Vacuum, Surfaces, and Films*, vol. 31, no. 1, pp. 01A116, 2013. [DOI: 10.1116/1.4764889]
19. Saha, D., Ajimsha, R. S., Rajiv, K., Mukherjee, C.,

Gupta, M., Misra, P. and Kukreja, L. M., "Spectroscopic ellipsometry characterization of amorphous and crystalline TiO_2 thin films grown by atomic layer deposition at different temperatures", *Appl. Surf. Sci.*, vol. 315, pp. 116-123, 2014. [DOI: 10.1016/j.apsusc.2014.07.098]

20. Y. Q. Wang and J. Y. Cai, "Enhanced cell affinity of poly (L-lactic acid) modified by base hydrolysis: Wettability and surface roughness at nanometer scale", *Curr. Appl. Phys*., vol. 7, no. 1, pp. e108-e111, 2007. [DOI: 10.1016/j.cap.2006.11.027]
21. Abubakar, S. and Yilmaz, E., "Optical and electrical properties of E-Beam deposited TiO_2/Si thin films" *J. Mater. Sci.: Materials in Electronics*, vol. 29, no. 12, pp. 9879-9885, 2018. [DOI: 10.1007/s10854-018-9029-9]
22. Kim, H., Yang, S., Park, K., Shanmugam, P. and Kwon, J. Y., "Leakage current analysis depends on grain size variation in zinc oxide thin film transistor", *J. Electrochem. Soc. Meet. Abstr. MA2013-02 76*, 2013.
23. Theivasanthi, T. and Alagar, M., "Titanium dioxide (TiO2) nanoparticles XRD analyses: an insight", *arXiv: 1307.1091*, 2013. [DOI: 10.48550/arXiv.1307.1091

접수일: 2023년 6월 4일, 심사일: 2023년 6월 16일,
게재확정일: 2023년 6월 21일